Journal of Magnetic Resonance 208 (2011) 256–261

Contents lists available at ScienceDirect

Journal of Magnetic Resonance

journal homepage: www.elsevier.com/locate/jmr

Diffusion exchange NMR spectroscopy in inhomogeneous magnetic fields

Oliver Neudert, Siegfried Stapf, Carlos Mattea *

Fachgebiet Technische Physik II/Polymerphysik, Institute of Physics, Technische Universität Ilmenau, PO Box 100 565, 98684 Ilmenau, Germany

ARTICLE INFO

Article history:
Received 18 August 2010
Revised 11 November 2010
Available online 21 November 2010

Keywords:
NMR diffusometry
Exchange
Low-field NMR
Porous media
Dynamics in porous media

ABSTRACT

Two-dimensional diffusion exchange experiments in the presence of a strong, static magnetic field gradient are presented. The experiments are performed in the stray field of a single sided NMR sensor with a proton Larmor frequency of 11.7 MHz. As a consequence of the strong and static magnetic field gradient the magnetization has contributions from different coherence pathways. In order to select the desired coherence pathways, a suitable phase cycling scheme is introduced. The pulse sequence is applied to study diffusion as well as the molecular exchange properties of organic solvents embedded in a mesoporous matrix consisting of a sieve of zeolites with a pore size of 0.8 nm and grain size of 2 μm. This pulse sequence extends the possibilities of the study of transport properties in porous media, with satisfying sensitivity in measurement times of a few hours, in a new generation of relatively inexpensive low-field NMR mobile devices.

1. Introduction

Diffusion measurements provide important insight into the study of molecular transport and dynamics in porous media. Molecular self-diffusion in fluids under confinement is a transport property that has been studied extensively by NMR (see [1] for an overview). In the last two decades the development of correlation spectroscopy in the time domain [2,3] has extended the possibilities to describe dynamical processes like diffusion and exchange in more detail. The introduction of a reliable algorithm for the inversion of the Laplace transform (ILT) in two dimensions [4] facilitated the analysis and interpretation of these kinds of experiments. The possibility of measuring diffusion in the stray field of mobile, i.e. generally low-field, NMR devices in a short time and in a reliable way was demonstrated recently in a number of papers [2,5]. The main difficulty in the presence of strong magnetic field inhomogeneities (or gradients) lies in the fact that the radio frequency (RF) pulses generate a set of unwanted coherences that have to be suppressed by appropriately cycling the phase of each pulse [6]. The conventional stimulated echo sequence for the diffusion experiment in presence of a strong constant magnetic field gradient requires a minimum of 16 scans [2]. Two-dimensional or even more complex pulse sequences normally require a more careful design of a phase cycle in order to both suppress unwanted pathways and optimize the time required for the experiment.

In this article, a two-dimensional diffusion–diffusion (D–D) exchange spectroscopy pulse sequence using a constant magnetic field gradient (Fig. 1) is introduced, to the knowledge of the authors, for the first time. A similar pulse sequence is known as DEXSY, which is based on Pulsed Field Gradients (PFG) [7]. Two stimulated echoes are applied in order to independently encode the molecular displacement during two defined intervals, separated by a mixing or exchange time t_{exch}. The phase cycling was designed in order to select the desired coherence pathways (see Fig. 1).

In contrast to the NMR D–D correlation experiments reported in the literature so far [7–9] that are based on pulsed field gradients, the experiment presented in this work possesses the advantage that it can be applied in grossly inhomogeneous magnetic fields. Regarding the recent development in portable magnets this is particularly advantageous as it widens the spectrum of their possible applications involving all the benefits they comprise, like low cost, possibility of measuring larger samples or to perform in situ studies. Moreover, the technique can be used as well in the stray fields of superconducting magnets to provide access to very short exchange times and/or to very small diffusion coefficients not being accessible otherwise. However when the samples consist of any sort of porous media, susceptibilities effects at high magnetic fields give rise to internal gradients that have to be taken into account in the interpretation of the results.

The feasibility and performance of the pulse sequence is demonstrated for a non-exchanging bulk phantom and for the case of exchange and diffusion of the organic solvent *n*-hexane adsorbed in a polycrystalline packing of zeolite cages. The analysis of the results is carried out twofold, both with ILT and directly in the time domain. A Monte Carlo simulation of the exchange process is performed and is used to support the analysis of the experimental data.

* Corresponding author. Fax: +49 3677693770.
E-mail address: carlos.mattea@tu-ilmenau.de (C. Mattea).

1090-7807/$ - see front matter © 2010 Elsevier Inc. All rights reserved.
doi:10.1016/j.jmr.2010.11.014

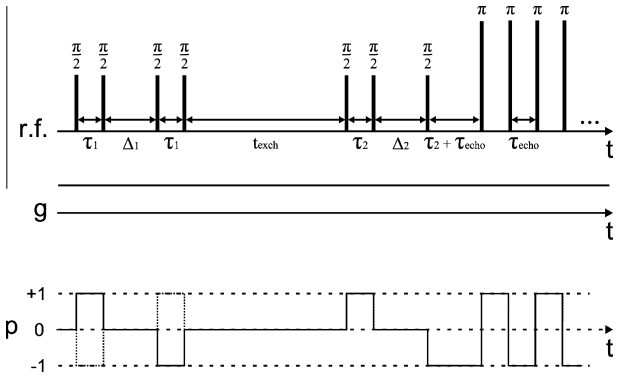

Fig. 1. (Top) Two-dimensional diffusion exchange (D–D) pulse sequence in the presence of a constant static magnetic field gradient (g). Radio frequency (RF) pulses are denoted by π and $\frac{\pi}{2}$. The time constants are defined in the text. (Bottom) Both the solid and the dotted lines represent desired coherence pathways.

2. Experimental

The diffusion–diffusion correlation pulse sequence is based on two successive stimulated echo (STE) pulse sequences separated by the interval t_{exch}, defining the time scale for exchange (see Fig. 1). The STE-parts are characterized by the two independently varied encoding times τ_1 and τ_2. The constant times Δ_1, Δ_2 define the timescales of the diffusion measurements. The last part is the CPMG pulse sequence with an echo time of τ_{echo} where the train of echoes is acquired and added up in order to increase sensitivity.

The combination of two separated stimulated spin echoes (STE) with an exchange interval (t_{exch}) includes as many as seven 90°-pulses. This requires the design of an adequate cycling of the phases for each RF-pulse. A phase cycling of 128 steps was introduced in order to select the two particular coherence pathways shown in the bottom part of Fig. 1. The development and optimization of the phase cycling was accomplished using the program CCCPv1.1 [10]. This program is able to simulate phase cycles in PFG NMR experiments and calculates selected pathways as well as their attenuations. As an approach to simulate the phase cycle in the experiments, gradient pulses of constant amplitude were assumed during the whole duration of each time interval in the pulse sequence. The coherence pathways were simulated up to the second stimulated echo (excluding the CPMG part). Then the step number per cycle, for each pulse, were optimized to achieve an effective phase cycle that is as short as possible whilst providing the best possible attenuation of unwanted coherence pathways. Especially in some critical situations (e.g. in the case when the encoding time has to account for fast diffusion processes and all time intervals are short or in the case when the STE parts are symmetric, i.e. $\tau_1 = \tau_2$ and $\Delta_1 = \Delta_2$) many different pathways can regain high phase coherence at the acquisition interval and therefore the signal is considerably disturbed. A phase cycle of 128 steps turned out to be sufficient for the attenuation of unwanted coherence pathways and the phase cycle scheme given in Table 1 was found to be the optimum for these number of steps.

The experiments were performed using the stray field of a single sided NMR spectrometer (profile NMR-MOUSE, ACT GmbH, Germany) with a ^{1}H resonance frequency of 11.7 MHz providing a time-constant magnetic field gradient of 11.5 T/m in the sensitive volume. The magnet and sample are kept at room temperature within 0.5 °C. The temperature of the magnet was monitored during the whole process, possessing a variation of ±0.5 °C. At the position of the sample, a minor increase in the temperature was detected due to the heating of the RF coil. This heating was well below 0.5 °C and did not significantly affect the diffusion process.

Two sets of samples are used. The first set is composed of two non-exchanging fluid phases filled into two concentric glass-cylinders. Two different preparations are used in this case, called **A1** and **A2**. For both of them the inner cylinder was filled with water. For sample **A1**, the outer cylinder was filled with a 70% solution of glycerol in water, while only glycerol was used for sample **A2**. $CuSO_4$ was added to the water compartment to reduce T_1 below 100 ms in order to shorten the measurement time. The bulk diffusion coefficients measured with a STE pulse sequence, are $D_{glyc\text{-}wat} = (1.07 \pm 0.03) \times 10^{-10}$ m^2/s, $D_{glyc} = (1.83 \pm 0.08) \times 10^{-11}$ m^2/s and $D_{water} = (2.5 \pm 0.1) \times 10^{-9}$ m^2/s. Sample **B** is based on a zeolite 13X porous sieve purchased from Sigma Aldrich Chemie GmbH, Germany (Catalog Number 283592) consisting of grains with an average diameter of around 2 μm and an inner pore size of 0.8 nm [11]. The porosity is found in literature; however the reported values differ to each other. Ref. [12] reports a porosity of 58% for Zeolites type X (with an error of 13.8%), while in Ref. [13] the value is 0.293. The mean particle size and porosity will be determined below by comparison of the experimental and simulated data. In order to eliminate residual water content, the zeolite was kept at 150 °C for 70 h. The porous sieve of zeolites was put into a glass vial filled with liquid n-hexane, shaken for several minutes and subsequently centrifuged to ensure a high packing density of the grains. As a result a bimodal pore structure is created, with two kinds of interconnected porous spaces, the mesoporous phase composed of grains of zeolites, and the inter-grain space with a characteristic pore space of the order of several micrometers. The NMR relaxation times T_1 and T_2 as well as the diffusion coefficient of n-hexane confined inside the zeolite sieves are shown in Table 2.

3. Simulation

A Monte Carlo simulation of the transport dynamics of a fluid in a model porous medium composed of packed spheres was developed in order to predict the NMR response to the exchange process that takes place inside the porous sample **B**. The comparison with the experimental data provides valuable insights of both, geometrical and dynamical properties of the system in sample **B**. Within

Table 2
NMR relaxation times and diffusion coefficient of n-hexane in sample **B** at room temperature. T_1 is measured with the saturation recovery pulse sequence. $T_{2,\text{eff}}$ is measured with a CPMG pulse sequence with an echo time of 53.5 μs.

	n-Hexane Bulk	n-Hexane Inter-particles	n-Hexane Intra-particles
T_1 (ms)	2160 ± 10		18.8 ± 0.6
$T_{2,\text{eff}}$ (ms)	67 ± 3	48 ± 3	9 ± 1
D ($\times 10^9$ m^2/s)	4.56 ± 0.01[a]	3.55 ± 0.05[b]	0.04 ± 0.01[b]

[a] Measured with 1-d STE pulse sequence.
[b] Diffusion constants obtained fitting Eq. (1) as is explained in the text. All measurements were done with the profile NMR-MOUSE device at 11.7 MHz.

Table 1
Phase cycle scheme and acquisition phase for the D–D exchange spectroscopy pulse sequence. All 180° pulses in the CPMG acquisition segment have the same phase. The acquisition phases were adjusted according to the cycling of the 90° pulses.

Pulse	90° #1	90° #2	90° #3	90° #4	90° #5	90° #6	90° #7	180°	Acq.
First phase	+x	+x	+x	+x	+x	+x	+x	+y	−x
Cycling steps	2	2	1	2	4	1	4	1	

this model the zeolite powder bed is described by two phases with different diffusion coefficients, which involves a coarse grain approximation of the zeolite's inner structure: Due to the small inner pore size of the zeolite, the effect of the geometrical confinement on the diffusion of hexane molecules can be described by a motionally averaged diffusion coefficient. The inner porosity of the spheres is set to 30% (see below). The powder bed was modeled by a close random packing of non-overlapping spheres with a narrow lognormal distribution of radii, and a packing density of 56.3%. Randomly packed ensembles were generated with 30 particles with a mean radius of 2 μm placed within a box with periodic boundary conditions, the size of the simulation space was 12 μm. A three-dimensional lattice was generated from these ensembles by discretizing into 300^3 cubic elements. At the beginning of the random walk simulation 100 molecules were randomly placed within the lattice according to this relation:

$$\frac{N_{in}}{N_{out}} = \frac{(1-\phi_{out})\phi_{in}}{\phi_{out}},$$

where N_{in} and N_{out} are the number of molecules inside and outside the cages respectively, ϕ_{in} denotes the (inner) porosity of the zeolite particle and ϕ_{out} denotes the outer porosity which is given by the packing density, $1-\phi_{out}$. The random walk was performed by independent discrete steps of length 1/300 in each dimension and for each molecule with a probability P_{step}. This probability corresponds to the diffusion coefficient depending on the current position of the molecule (inside or outside of a zeolite particle). After each simulation step involving the movement of all molecules, the number of molecules inside the particles was checked and compared with the initial value. Simulation steps for which the number of molecules inside the particles exceeded a deviation of 5% were rejected and repeated. The outputs started to be recorded after 100 simulation steps from the beginning of the simulation in order to allow the system to reach a steady state.

The main outputs of this simulation are the assignment to either inter- or intra-particle phase of each molecule at every timestep. From this information the exchange probabilities are computed by counting the number of molecules that started in one defined phase and ended up in another defined phase after a variable number of simulation steps. By monitoring these numbers, the pure exchange process can be studied.

The effect of NMR longitudinal relaxation on the signal during the experiment was considered by assigning a factor to each molecule that was multiplied by $e^{-\frac{\Delta t}{T_{1,i}}}$ at each timestep Δt. The relaxation time $T_{1,i}$ was chosen depending on whether the molecule was currently inside or outside a particle for which the relaxation times $T_{1,in}$ and $T_{1,out}$ were assumed, respectively. They were chosen according to Table 2. The above mentioned number of exchanged and non-exchanged molecules was then weighted by these factors.

The relaxation-weighted number of molecules is directly compared to the parameters a_{ij} from the time-domain fitting (see Fig. 5). The simulations were performed with the software Matlab.

4. Results and discussions

The pulse sequence was tested employing samples **A1** and **A2**, where the two liquids are not able to physically exchange. The

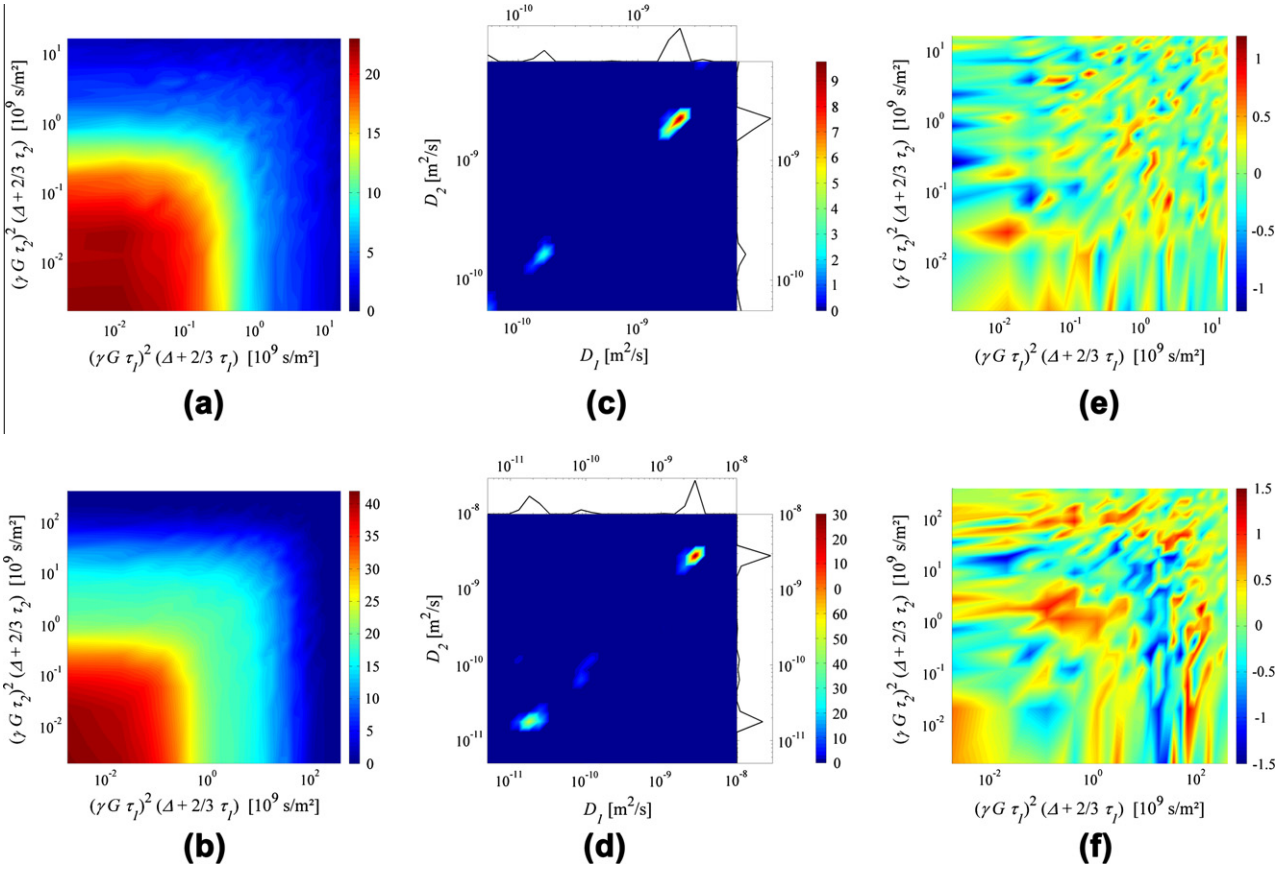

Fig. 2. D–D measurement of the test samples **A1** and **A2**. (a and b) Echo decays in the 2-d time domain for sample **A1** (a) and sample **A2** (b). (c and d) Diffusion spectrum from 2-d Laplace inversion for sample **A1** (c) and sample **A2** (d). The two peaks in (c) coincide with the bulk diffusion constants of the glycerol–water mixture and water, while the two peaks in (d) coincide with the bulk diffusion constants of the glycerol and water. (e and f) Residuals of the fitting of the echo decays with Eq. (1). (e) Corresponds to sample **A1** and (f) to sample **A2**. The relevant experimental parameters in the pulse sequence are τ_1, τ_2 = from 7.0 μs to 0.6 ms; Δ_1, Δ_2 = 4 ms for sample **A1** and τ_1, τ_2 = from 7.0 μs to 2.7 ms; Δ_1, Δ_2 = 4.0 ms for sample **A2**. The magnitudes can be compared by inspection of the color bars.

two-dimensional echo decays $S(\tau_1, \tau_2)$ are shown in Fig. 2a and b. The data were analyzed using the following approaches: First an Inverse Laplace inversion algorithm developed by Venkataramanan et al. [4] is applied on the two-dimensional experimental echo decays $S(\tau_1, \tau_2)$ in order to obtain a 2-d D–D spectrum. Two diagonal peaks are obtained as expected (Fig. 2c and d). The positions of the peaks coincide with the results obtained performing a 1-d STE experiment with the same sample.

For both samples **A1** and **A2**, the intensities of each peak correspond to the relaxation-weighted relative amount of protons in these two phases. The magnitudes of the peak integrals were compared with the component amplitudes obtained from the 1-d STE experiment. This comparison showed nice agreement for the ratios of both peak integrals and component amplitudes after correcting for longitudinal relaxation.

The D–D spectrum in Fig. 2d, corresponding to sample **A2**, shows a spurious peak of low intensity on the diagonal at $D_{1,2} = 10^{-10}\ \mathrm{m^2 s^{-1}}$. This peak has no physical meaning and arises due to the fact that the longest encoding time is on the order of T_2. The attenuation factor due to the relaxation time T_2 in the echo decays is $\exp(-\xi\tau_1/T_2)$ where the coefficient ξ is 2 or 4 depending whether the experiment is 1-d STE or 2-d D-D, respectively. The influence of T_2 on the measured diffusion coefficients is therefore negligible when the condition for the longest encoding time, $\xi\tau_{1,longest} \ll T_2$ is satisfied. In both samples **A1** and **B**, the shortest T_2 relaxation time satisfies this condition, while in the case of sample **A2** a long encoding time τ_1 is needed in order to measure the low diffusion coefficient of the glycerol phase.

When the number and approximate position of the peaks is known, $S(\tau_1, \tau_2)$ is fitted with the following function [9]

$$S_{fit}(\tau_1, \tau_2) = \sum_{i,j=1}^{2} a_{ij} \exp(-q_1 D_i) \exp(-q_2 D_j), \quad (1)$$

where $q_{1,2} = g^2\gamma^2\tau_{1,2}^2\left(\frac{2}{3}\tau_{1,2} + \Delta_{1,2}\right)$. The coefficients a_{ii} are proportional to the number of molecules in each phase while $a_{i\neq j}$ are proportional to the molecules that have exchanged (see below). The residual matrix $S_{res} = S - S_{fit}$ is used to check the validity of the fit model. Fig. 2c and f shows the residuals. They are sufficiently uniformly distributed, i.e. no specific pattern can be distinguished. The analysis of the data was done with the software Matlab and Origin. The diffusion coefficients found by fitting with Eq. (1) are $D_{glyc\text{-}wat} = (1.6 \pm 0.5) \times 10^{-10}\ \mathrm{m^2/s}$, $D_{glyc} = (1.7 \pm 0.7) \times 10^{-11}\ \mathrm{m^2/s}$ and $D_{water} = (2.5 \pm 0.6) \times 10^{-9}\ \mathrm{m^2/s}$. They coincide inside the experimental error with the results obtained using a 1-d STE pulse sequence.

In order to investigate the importance of artefacts, a D–D experiment was carried out with an incomplete phase cycling in the test sample **A2**. A single STE phase cycle is done in the first STE-part of the D–D pulse sequence. Fig. 3a shows the two-dimensional echo decay, $S(\tau_1, \tau_2)$. Note that the distribution of the absolute intensities is different from that of Fig. 2a. The Inverse Laplace algorithm is applied and the results shown in Fig. 3b. Note the presence of extra (more than two) peaks on the diagonal and the dominating peak on the edge at high diffusion coefficients. These effects are explained by the survival of unwanted coherences due to the use

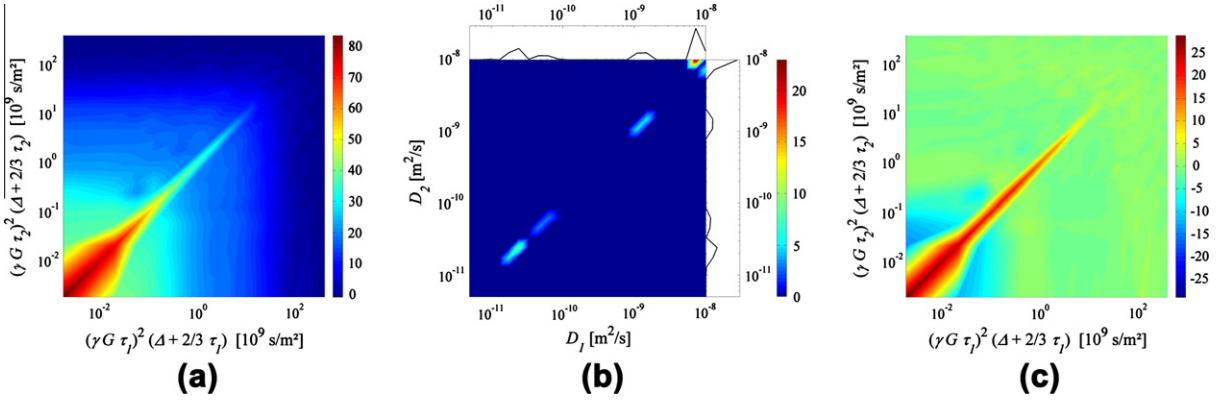

Fig. 3. D–D measurement of sample **A2** with the incomplete phase cycling. (a) Echo decays in the 2-d time domain. (b) Diffusion spectrum from 2-d Laplace inversion. The peak corresponding to the longest encoding times coincides with the bulk diffusion constants of glycerol, while the peak related with the higher diffusion coefficient/short encoding times, is affected as explained in the text. (c) Residuals of the fitting of the echo decays with Eq. (1). The magnitudes can be compared by inspection of the color bars.

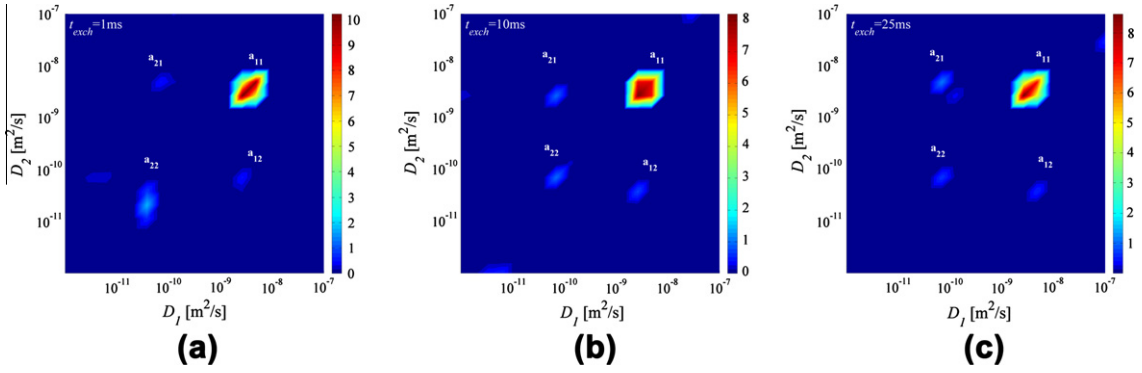

Fig. 4. D–D diffusion spectra of sample **B** obtained from Laplace inversion of the echo decays for the three different exchange times 1 ms (a), 10 ms (b) and 25 ms (c). The relevant experimental parameters in the pulse sequence are τ_1, τ_2 = from 5.5 μs to 0.75 ms; Δ_1, Δ_2 = 1.6 ms. The factors $a_{i,j}$ correspond to the intensity of the peaks as explained in the text. The presence of the off-diagonal peaks, $a_{i\neq j}$, is the signature of the exchange process present in the sample.

of an incomplete phase cycle. The artefacts in the data become more evident when the fitting with the function S_{fit} is done and the residuals are plotted (Fig. 3c). Note that the errors are more relevant for shorter encoding times. In consequence, the values of the larger diffusion coefficient are more affected than the lower value in Fig. 3b.

Fig. 4 shows the result of the D–D correlation experiment of *n*-hexane confined in the bimodal porous sample **B**. It presents three ILT maps at different evolution times t_{exch}. The two diagonal peaks show a distribution of diffusion constants corresponding to the diffusion of the solvent molecules in the intra- and inter-particle phases. The respective areas of these peaks are proportional to the population of molecules that either did not exchange, or have returned to their initial phase, during the corresponding t_{exch} period. The diffusion coefficients at the center of each peak correspond to that diffusion coefficients obtained when the single STE experiment is used and there is a good agreement with literature values for this solvent using PFG diffusometry [14]. The off-diagonal peaks reveal the presence of exchange of the solvent molecules between the different phases of the porous sample. The peak a_{12}, for instance, corresponds to the molecules that, during t_{exch}, started in the inter-particle space and ended inside the zeolite particles. It can be seen in these figures that at longer waiting times, the relative intensities of the diagonal peaks decrease, while the intensities of the off-diagonal peaks do increase. The apparent imbalance of the intensities of the $a_{i\neq j}$ coefficients observed for t_{exch} = 25 ms is a consequence of the experimental errors. Dynamical equilibrium requires identical intensities in the off-diagonal peaks.

As mentioned above, the experimental data are analyzed both in the time domain and with ILT. The coefficients a_{ij} are proportional to the areas under the peaks. a_{ij} coefficients as well as the diffusion constants $D_{1,2}$ are in agreement with both analytical procedures. The advantage of that procedure is a better fidelity of the results, knowing that the ILT algorithm is quite sensitive to artefacts. These coefficients reveal both the exchange dynamics as well as the T_1 NMR relaxation process present in the sample. This is a general statement for any 2-d exchange experiment (see for instance Ref. [15]).

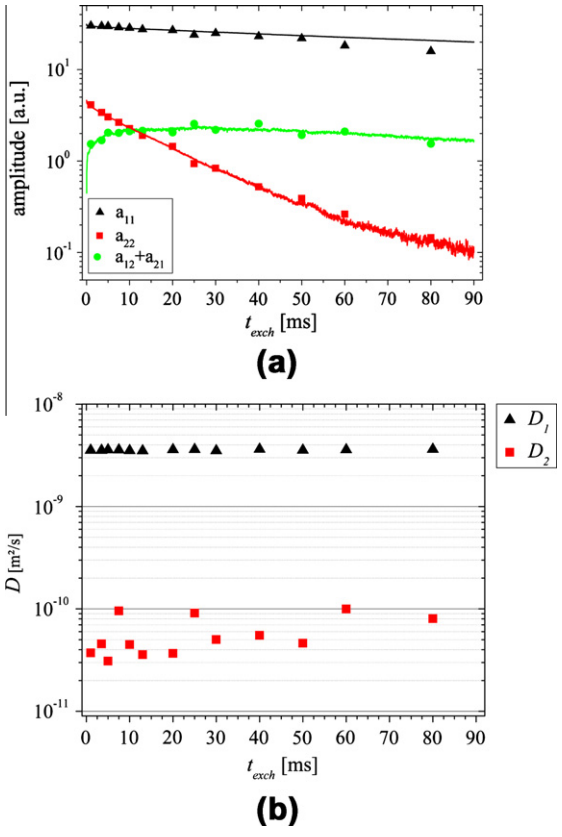

Fig. 5. (a) The symbols correspond to the amplitude factors $a_{i,j}$ obtained from the time-domain fitting of the exchange experiments of sample **B**. The full lines correspond to the relaxation-weighted exchange probabilities obtained by the Monte Carlo simulation. The simulation parameters were adjusted to fit the experimental data. (b) Diffusion coefficients $D_{1,2}$ obtained from the time-domain fitting in function of the exchange time.

Fig. 5a shows the amplitude factors a_{ij} obtained from the time-domain fitting of the exchange experiments of sample **B**, in function of the exchange time. The signature of a T_1 relaxation processes present in the sample are seen in the decay of the amplitude coefficients when the exchange process is progressing. It can be seen as well the agreement with the simulated exchange-coefficients in function of t_{exch}. The difference in the rate of the decay of the diagonal exchange-coefficients a_{11} and a_{22}, showing a less effective averaging of the relaxation time for a_{22}, can be explained assuming a higher exchange time for molecules that have started closer to the center of the zeolite particles. This situation is taken into account in the Monte Carlo simulation. The details will be given elsewhere [16].

The signal to noise ratio for sample **B** is around 90 for the lowest exchange times, above 70 for intermediate times and 42 for the lowest exchange time of 80 ms. 256 echoes were acquired and 256 averages were used for each combination of encoding times. Even though the changes in amplitude are small, they are systematic upon the variation of the exchange time (Fig. 5a). Furthermore their amplitude is always above the noise level of around 0.4 intensity units, calculated from the root of the mean squared residuals.

The fits of the diffusion coefficients with the function (1) for the different exchange times are shown in Fig. 5b. The regularity in the D_1 values reflects the good sensitivity in the measurement of high diffusion coefficients, while the scatter observed in the D_2 values originates in the limitations of the encoding time satisfying the condition $2\tau_{1,2} + \Delta_{1,2} < t_{exch}$.

The mean particle radius and porosity are determined by only adjusting these two parameters in the simulation in order to obtain a good agreement with the experimental results as it is shown in Fig. 5. The parameter corresponding to the porosity was set ϕ_{in} = 30%, in good agreement with the value of 29.3% reported in Ref. [13], and the mean particle radius $\langle r \rangle$ = 2 μm.

In T_1 measurements and especially in $T_1 - D$ measurements (not shown here) two components can be distinguished (see Table 2). These components are attributed to T_1 of the *n*-hexane molecules inside the zeolite particles and the motional averaged $T_{1,\text{eff}}$. T_1 in the inter-particle region cannot be measured because this relaxation takes much longer than the exchange process. This relaxation time is assumed to be close to the bulk value around 2.2 s.

5. Conclusions

Diffusion–diffusion exchange experiments using the stray field of a magnet with low magnetic field B_0 and a strong magnetic field gradient was successfully introduced by employing a suitable phase cycling scheme to suppress unwanted coherence pathways which are of detrimental influence in grossly inhomogeneous fields. The pulse sequence was applied to study the molecular exchange between two different environments of a fluid inside a porous media. The experiments were analyzed by Inverse Laplace Transform as well as in the time domain with the help of a function describing two-phase exchange. The agreement between the set of fitted parameters in the time domain and the two-dimensional maps (intensities of the peaks) validate the measurements and the applied model. The results were further corroborated by Monte

Carlo simulations of the dynamics of the solvent molecules inside the porous media. Analysis of these simulations successfully rendered the characteristic dimensions and dynamics parameters of the system. It can thus be concluded that the presented method is able to provide a versatile, robust and reliable access to quantifying exchange processes in two- and potentially multi-component diffusion systems with a mobile NMR device.

Acknowledgment

We thank Y.-Q. Song for providing the code for the 2D ILT routine.

References

[1] W. Price, NMR Studies of Translational Motion, Cambridge Univ. Press, 2009.
[2] M.D. Hürlimann, L. Venkataramanan, Quantitative measurement of two-dimensional distribution functions of diffusion and relaxation in grossly inhomogeneous fields, J. Magn. Reson. 157 (2002) 31.
[3] J. Lee, C. Labadie, C. Springer Jr., G. Harbison, Two-dimensional Inverse Laplace transform NMR: altered relaxation times allow detection of exchange correlation, J. Am. Chem. Soc. 115 (1993) 7761.
[4] L. Venkataramanan, Y.-Q. Song, M.D. Hürlimann, Solving Fredholm integrals of the first kind with tensor product structure in 2 and 2.5 dimensions, IEEE Trans. Signal Process 50 (2002) 1017.
[5] D.G. Rata, F. Casanova, J. Perlo, B. Blümich, Self-diffusion measurements by a mobile single-sided NMR sensor with improved magnetic field gradient, J. Magn. Reson. 180 (2006) 229.
[6] M. Hürlimann, Diffusion and relaxation effects in general stray field NMR experiments, J. Magn. Reson. 148 (2001) 367.
[7] P.T. Callaghan, I. Furó, Diffusion–diffusion correlation and exchange as a signature for local order and dynamics, J. Chem. Phys. 120 (2004) 4032.
[8] Y. Qiao, P. Galvosas, P.T. Callaghan, Diffusion correlation NMR spectroscopic study of anisotropic diffusion of water in plant tissues, Biophys. J. 85 (2005) 2899.
[9] Y. Qiao, P. Galvosas, T. Adalsteinsson, M. Schönhoff, P.T. Callaghan, Diffusion exchange NMR spectroscopic study of dextran exchange through polyelectrolyte multilayer capsules, J. Chem. Phys. 122 (2005) 214912.
[10] A. Jerschow, N. Müller, Efficient simulation of coherence transfer pathway selection by phase cycling and pulsed field gradients in NMR, J. Magn. Reson. 134 (1998) 17.
[11] H. van Bekkum, E. Flanigen, P. Jacobs, J. Jansen (Eds.), Introduction to Zeolite Science and Practice, Second ed., Elsevier, 2001.
[12] S. Huang, Y. Yu, T. Lee, T. Lu, Correlations and characterization of porous solids by fractal dimension and porosity, Physica A 274 (1999) 419.
[13] F. Rittig, C. Coe, J. Zielinski, Pure and multicomponent gas diffusion within zeolitic adsorbents: pulsed field gradient NMR analysis and model development, J. Phys. Chem. B 107 (2003) 4560.
[14] J. Kärger, G. Seiffert, F. Stallmach, Space- and time-resolved PFG NMR self-diffusion measurements in zeolites, J. Magn. Reson. A102 (1993) 327.
[15] M. Van Landeghem, A. Haber, J.-B.D. de Lacaillerie, B. Blümich, Analysis of multisite 2D relaxation exchange NMR, Concepts Magn. Reson. 36A (2010) 153.
[16] O. Neudert, S. Stapf, C. Mattea, New J. Phys., submitted for publication.